Numerical simulation of Raman resonance due to the Ramsey interference induced by thermal motion of atoms

2009 Phys. Scr. 2009 014026

(http://iopscience.iop.org/1402-4896/2009/T135/014026)

Phys. Scr. **T135** (2009) 014026 (5pp) doi:10.1088/0031-8949/2009/T135/014026

Numerical simulation of Raman resonance due to the Ramsey interference induced by thermal motion of atoms

Zoran Grujić, Dušan Arsenović, Milan Radonjić, Marina Mijailović and Branislav Jelenković

Institute of Physics, Pregrevica 118, Belgrade, Serbia

E-mail: zoran.grujic@phy.bg.ac.yu

Received 21 January 2009
Accepted for publication 22 January 2009
Published 31 July 2009
Online at stacks.iop.org/PhysScr/T135/014026

Abstract

We use the optical Bloch equations to calculate spontaneous emission and Zeeman coherences of the probe laser beam in coaxial pump–probe configuration in rubidium (Rb) vapor. To properly model the open $F_g = 2 \rightarrow F_e = 1$ transition, the solution of the time-dependent optical Bloch equations was necessary. Also, due to the nature of a room temperature Rb vapor, we performed averaging of the total population of the excited $F_e = 1$ state over different atomic velocities according to the Maxwell–Boltzmann distribution and over different directions of propagation of atoms through pump and probe laser beams. Time-dependent diagonal and nondiagonal density matrix elements for atoms are presented and discussed.

PACS numbers: 42.50.Gy, 42.50.Nn, 42.65.−k

(Some figures in this article are in colour only in the electronic version.)

1. Introduction

The search for better sensors leads scientists to study atoms and their interaction with light. Use of cells with alkali vapor introduces simple but powerful and cheap tools for atomic spectroscopy. The properties of coherently prepared media ([1] and references therein) have attracted great attention. Electromagnetically induced transparency (EIT) ([2] and references therein) has been studied intensively. Narrow EIT structures have been obtained in buffer gas, pure rubidium (Rb) and cells with coherence-preserving wall coating.

In cells with coated walls, resonance narrowing is obtained thanks to reuse of coherently prepared atoms after many collisions with the cell wall [3]. Buffer gas limits the rate of atom diffusion out of the laser beam and allows the return of atoms back to the laser beam, thus considerably increasing the coherence buildup time [4].

The subject of this paper is the theoretical simulation of the interaction between atoms and two spatially separated laser excitation regions in a pure Rb vapor cell as a function of the axial magnetic field B. We use the hollow pump laser beam to create the coherence. This coherence was subsequently tested by calculated transmission of the copropagating probe beam located at its center. Inverse beam geometry has been used by Briaudeau *et al* [5] where the sub-Doppler feature was observed in the transmission of the hollow probe beam, through a very thin (10 μm) cell, whereas the pump beam is placed at the probe center.

2. Theory

Our model uses these assumptions:

1. In an uncoated pure Rb vapor cell, all atoms after collision with a cell wall reset their state, i.e. lose the coherence induced during previous interactions.
2. Our laser beam configuration has radial symmetry.
3. Atoms interact only with laser beams, magnetic field and cell walls due to low vapor pressure at room temperature, i.e. there is no collisions between atoms. This implies that atom trajectories are straight lines.
4. The vapor is in thermal equilibrium, i.e. the Maxwell–Boltzmann velocity distribution describes the motion of atoms in the cell.
5. The magnetic field is homogeneous and stationary $\vec{B}(\vec{r}, t) = \text{const}$.
6. Atom fluorescence is proportional to the excited-level population and is related to absorption.

2.1. The density matrix method

The transition $F_g = 2 \rightarrow F_e = 1$ at the ^{87}Rb D1 line is open (figure 1(a)). There are two possible deexcitation paths from the $F_e = 1$ level: to the coupled $F_g = 2$ and to the uncoupled $F_g = 1$ level. A configuration like this needs to be treated as time dependent in contrast to closed transitions where stationary solutions for the density matrix exist and could be used. So, we solve numerically the time-dependent optical Bloch equations:

$$\begin{aligned}
\dot{\varrho}_{e_i e_j} &= \varrho_{e_i e_j} i(\omega_{e_j} - \omega_{e_i}) + \frac{i}{\hbar} \sum_{k=-2}^{2} (\tilde{\varrho}_{e_i g_k} E_{+g_k e_j} - E_{-e_i g_k} \tilde{\varrho}_{g_k e_j}) \\
&\quad - 2\Gamma_L \varrho_{e_i e_j} \sum_{F'_g} \langle J_g \| e\vec{r} \| J_e \rangle^2 (2F'_g + 1)(2J_g + 1) \\
&\quad \times \begin{Bmatrix} J_g & J_e & 1 \\ F_e & F'_g & I_g \end{Bmatrix}^2, \\
\dot{\tilde{\varrho}}_{e_i g_j} &= \tilde{\varrho}_{e_i g_j} i(\omega - (\omega_{e_i} - \omega_{g_j})) \\
&\quad + \frac{i}{\hbar} \left(\sum_{k=-1}^{1} \varrho_{e_i e_k} E_{-e_k g_j} - \sum_{k=-2}^{2} E_{-e_i g_k} \varrho_{g_k g_j} \right) \\
&\quad - \Gamma_L \varrho_{e_i e_j} \sum_{F'_g} \langle J_g \| e\vec{r} \| J_e \rangle^2 (2F'_g + 1)(2J_g + 1) \\
&\quad \times \begin{Bmatrix} J_g & J_e & 1 \\ F_e & F'_g & I_g \end{Bmatrix}^2, \\
\dot{\varrho}_{g_i g_j} &= \varrho_{g_i g_j} i(\omega_{g_j} - \omega_{g_i}) + \frac{i}{\hbar} \sum_{k=-1}^{1} (\tilde{\varrho}_{g_i e_k} E_{-e_k g_j} - E_{+g_i e_k} \tilde{\varrho}_{e_k g_j}) \\
&\quad + 2\Gamma_L \langle J_g \| e\vec{r} \| J_e \rangle^2 (2F_g + 1)(2F_e + 1)(2J_g + 1) \\
&\quad \times \begin{Bmatrix} J_g & J_e & 1 \\ F_e & F_g & I_g \end{Bmatrix}^2 \\
&\quad \times \sum_{q=-1}^{1} \varrho_{e_{i+q} e_{j+q}} \begin{pmatrix} F_e & 1 & F_g \\ j+q & -q & -j \end{pmatrix} \\
&\quad \times \begin{pmatrix} F_e & 1 & F_g \\ i+q & -q & -i \end{pmatrix},
\end{aligned} \tag{1}$$

where

$$\begin{aligned}
E_{+a_i a_j} &= -\mu_{a_i a_j - 1} E_{-1+} - \mu_{a_i a_j 1} E_{+1+} - \tfrac{1}{2} \mu_{a_i a_j 0} \, e^{i\varphi^{zx}} E_{0z}, \\
E_{-a_i a_j} &= -\mu_{a_i a_j - 1} E_{-1-} - \mu_{a_i a_j 1} E_{+1-} - \tfrac{1}{2} \mu_{a_i a_j 0} \, e^{-i\varphi^{zx}} E_{0z}, \\
E_{-1+} &= \frac{E_{0x} + i e^{i\varphi^{yx}} E_{0y}}{2\sqrt{2}}, \\
E_{-1-} &= \frac{E_{0x} + i e^{-i\varphi^{yx}} E_{0y}}{2\sqrt{2}}, \\
E_{+1+} &= \frac{-E_{0x} + i e^{i\varphi^{yx}} E_{0y}}{2\sqrt{2}}, \\
E_{+1-} &= \frac{-E_{0x} + i e^{-i\varphi^{yx}} E_{0y}}{2\sqrt{2}},
\end{aligned} \tag{2}$$

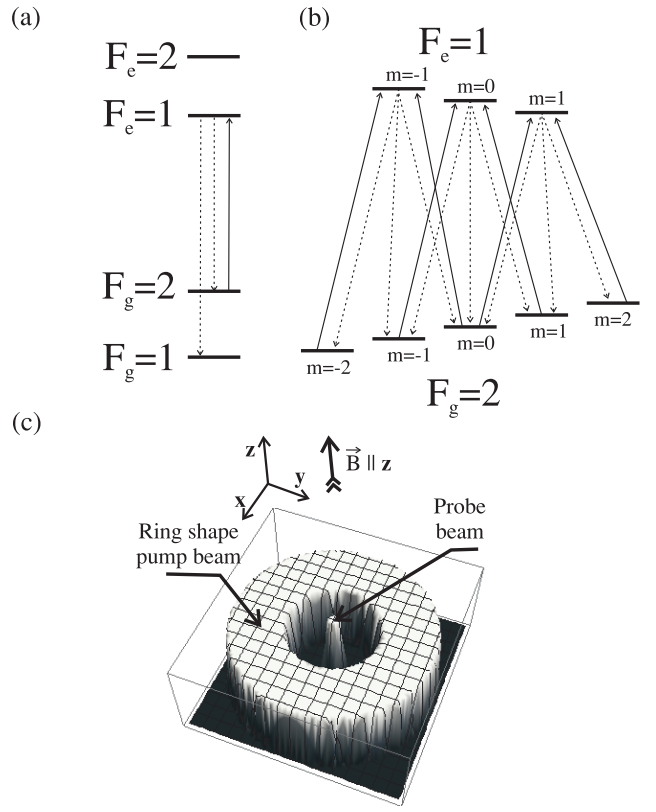

Figure 1. (a) Atomic energy level diagram for ^{87}Rb D1 line ground and excited levels, (b) the energy level diagram for magnetic sublevels of the $F_g = 2 \rightarrow F_e = 1$ transition and (c) pump and probe laser beam radial profiles used in the theoretical model. In (a) and (b), solid lines represent laser light coupling energy levels and dotted lines show the de-excitation paths from excited levels.

and $\mu_{a_i a_j q}$ is the matrix dipole element, and $\hbar\omega_{e_i}$ and $\hbar\omega_{g_i}$ are the energies of the Zeeman sublevels. Fast oscillations at the laser frequency in equation (1) were eliminated by common substitution $\varrho_{e_i g_j} = \tilde{\varrho}_{e_i g_j} \times e^{-i\omega t}$. The summation F'_g is over ground states $F_g = 1, 2$. E_{0x}, E_{0y} and E_{0z} are the x-, y-, z-components of the laser's electric vector and φ^{yx} and φ^{zx} are the corresponding phases. The laser beam propagation direction is along the z-axis.

$$\begin{aligned}
\vec{E} &= \vec{e}_x \cos \omega t \cdot E_{0x} + \vec{e}_y \cos(\omega t + \varphi^{yx}) \cdot E_{0y} \\
&\quad + \vec{e}_z \cos(\omega t + \varphi^{zx}) \cdot E_{0z}.
\end{aligned} \tag{3}$$

The identity

$$\sum_{F'_g} (2F'_g + 1) \begin{Bmatrix} J_g & J_e & 1 \\ F_e & F'_g & I_g \end{Bmatrix}^2 = \frac{1}{2J_e + 1} \tag{4}$$

relates Γ_L in equation (1) to the emission rate Γ

$$\Gamma = 2\Gamma_L \langle J_g \| e\vec{r} \| J_e \rangle^2 \frac{2J_g + 1}{2J_e + 1}. \tag{5}$$

Here, $\langle J_g \| e\vec{r} \| J_e \rangle^2$ is the reduced matrix element of the dipole operator between the ground and excited states [6].

As schematically given in figure 1(c), the probe laser beam propagates along the axis of the hollow pump beam. Both the pump and probe beams have the same frequency, ω.

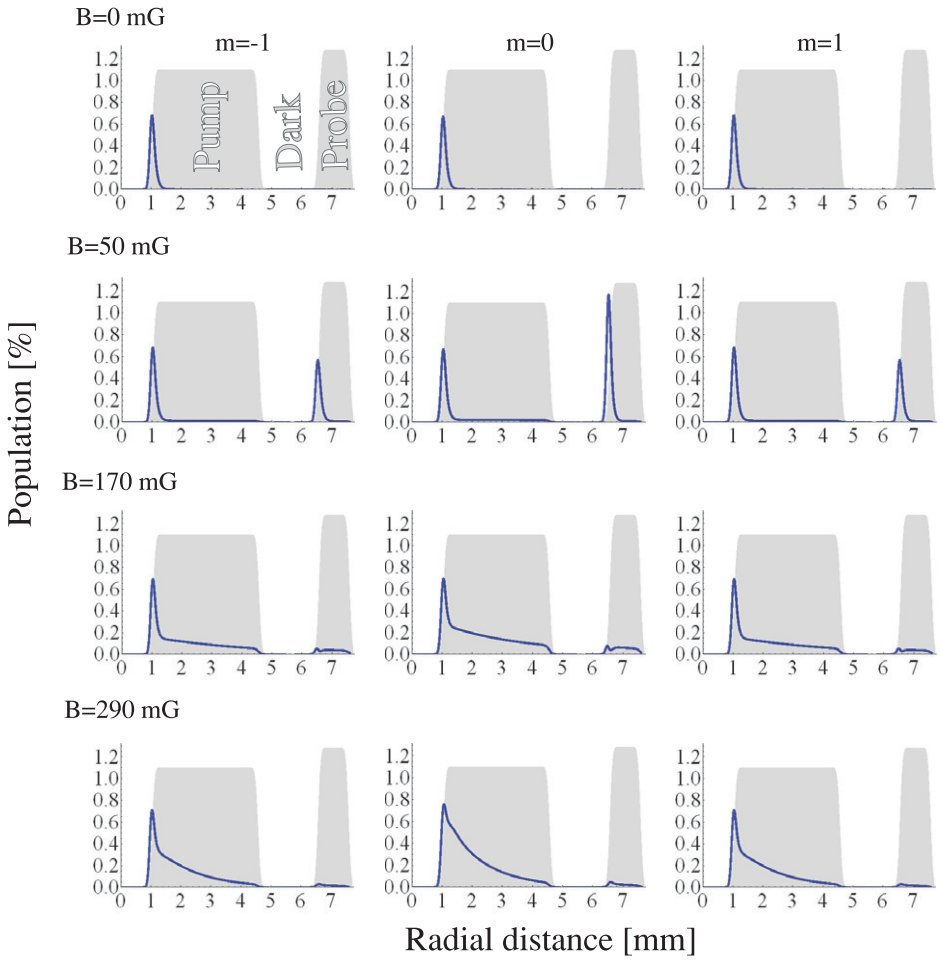

Figure 2. Calculated dependence of excited level populations as a function of the radial position of an atom (as the atom passes through the pump beam, the 'dark region' and the probe region) for different values of B. Columns: population of excited magnetic sublevels from left to right $m = -1, 0, 1$, respectively. Results are given for the magnetic field values of 0, 50, 170 and 290 mG, for four rows top to bottom and average pump and probe powers of 2 mW and 20 μW, respectively, for the atom velocity of 260 m s^{-1} and its trajectory along the probe beam diameter. The distances that atoms travel through the pump, 'dark' and probe regions are 3.5, 1.7 and 1.5 mm, respectively.

Their radial intensity profiles are modelled by

$$E(r) = \frac{\mathtt{Erf}\Big((r-r_1)/a(r_2-r_1)\Big) - \mathtt{Erf}\Big((r-r_2)/a(r_2-r_1)\Big)}{2}, \tag{6}$$

where r_1, r_2 and a are suitable parameters, and

$$\mathtt{Erf}(z) = \frac{2}{\sqrt{\pi}} \int_0^z \mathrm{e}^{-t^2} \mathrm{d}t. \tag{7}$$

Density matrix elements in equation (1) are functions of time, whereas the laser electric field amplitude is a function of the radial coordinate r (see equation (6)). We replace r in equation (6) with $v * t$, where v is the atom velocity. We assume that the atoms have straight trajectories and Maxwell–Boltzmann velocity distribution. We assume that the atoms pass through the center of the probe beam. Integration of equation (1) is performed from $t = 0$, or from the point where the atom enters the pump beam, while the atom is in the nonilluminated or precession region, and finally while the atom is in the probe beam. Integration is stopped when the atom leaves the probe beam.

Because the density matrix is Hermitian, this allow us to speed up the simulation by reducing the number of equations from $8 * 8 = 64$ to 36 with substitutions $\varrho_{\mathrm{e}_i\mathrm{e}_j} = \varrho_{\mathrm{e}_j\mathrm{e}_i}$, $\varrho_{\mathrm{g}_i\mathrm{g}_j} = \varrho_{\mathrm{g}_j\mathrm{g}_i}$ and $\tilde{\varrho}_{\mathrm{g}_i\mathrm{e}_j} = \tilde{\varrho}_{\mathrm{e}_j\mathrm{g}_i}$.

We first discuss some partial results shown in figures 2 and 3.

In figure 2, we show populations of the magnetic sublevels of the excited $F_\mathrm{e} = 1$ level. Polarizations of the pump and the probe beam are linear and parallel to each other. For $B = 0$, we see generation of the ideal dark state in the pump beam, after a short interaction, and then the atom stays in the dark state in the probe beam. This corresponds to the EIT or to the total medium transparency for the resonant probe light. For $B \neq 0$, the dark state is not ideally dark. As a result, the fluorescence of an atom in the pump beam or excited sublevel population increases with the magnetic field. In the probe beam, the spatial dependence of the fluorescence is different and strongly depends on the B. At $B = 0$ and $B = 170$ mG, we have none or low excited level population, but for $B = 50$ mG this population is high.

In figure 3, the first row shows the total $F_\mathrm{e} = 1$ level population, whereas on the second row the Zeeman coherence $\varrho_{\mathrm{g}_0\mathrm{g}_{-2}}$ has been shown. The phase of the coherence

$$\alpha = \arg\left(\varrho_{\mathrm{g}_0\mathrm{g}_{-2}}\right) \tag{8}$$

plays a key role in the interaction between atoms and the probe beam. If $\alpha = 0 + 2k\pi$, where k is an integer, the atoms

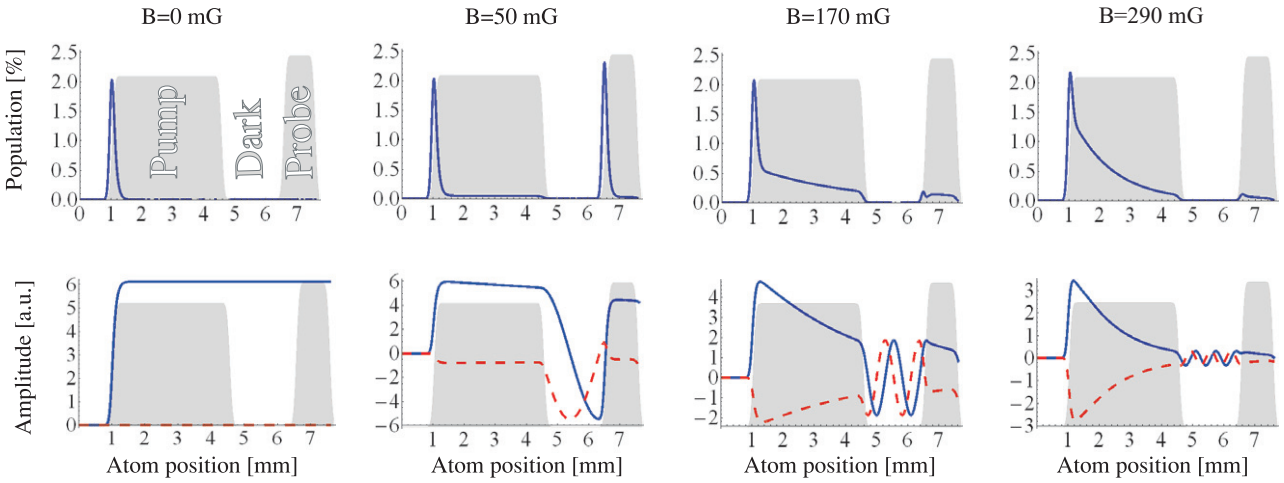

Figure 3. Calculated dependence of spontaneous emission and of ground-state coherence between the Zeeman sublevels as a function of the radial position of an atom (as the atom passes through the pump beam, the 'dark region' and the probe region) for different values of B. The first row: spontaneous emission from the excited $F_e = 2$ hyperfine level. The second row: the real (solid line) and imaginary (dashed line) parts of the Zeeman coherence induced between $m_F = 0$ and $m_F - 2$ Zeeman sublevels of $F_g = 2$. Beam powers and dimensions are the same as in figure 2.

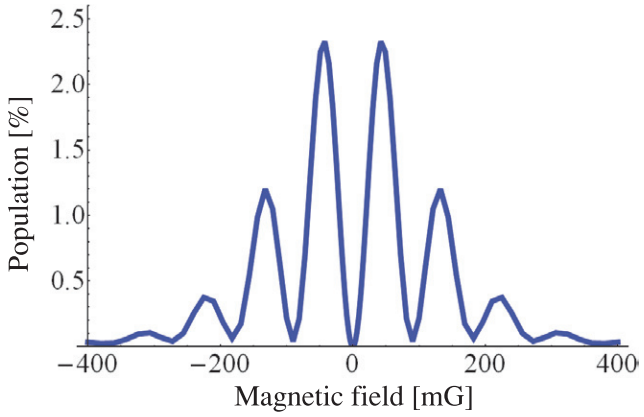

Figure 4. Calculated dependence of spontaneous emission for atoms with a velocity of 260 m^{-1} s at the entrance into the probe beam. Beam powers and dimensions are the same as in figure 2.

do not interact with the resonant light, but for $\alpha = \pi + 2k\pi$ absorption is maximal. Coherence phase changes, in the 'dark region', could be approximated with

$$\Delta\alpha(t) = 2\pi \frac{2\mu_B g_F B}{h} t, \tag{9}$$

where μ_B is the Bohr magneton, g_F is the gyromagnetic factor of the level and h is the Planck constant. From this we may conclude that for atoms with the same velocity and for different magnetic fields B, the phase of the coherence and absorption in the probe beam will be different.

In figure 4, the total excited level population has been shown as a function of the axial magnetic field right after atoms enter the probe beam. The minima, in figure 4 are characteristic Ramsey fringes. But, in Rb vapor, atoms have Maxwell–Boltzmann velocity distribution. This will wash out higher order Ramsey fringes in the probe transmission.

2.2. Averaging

In this model, laser intensities and beam dimensions are inputs used to calculate the density matrix for an array of magnetic field values and an array of velocity vectors. The atom fluorescence is proportional to the total excited-state population

$$\Pi_e(t, B, \vec{v}) = \sum_i \varrho_{e_i e_i}(t, B, \vec{v}), \tag{10}$$

where $\vec{v}$ is the atom velocity vector. The total fluorescence from an atom due to excitation by the probe beam is

$$I_e(B, \vec{v}) = \int_{t_i}^{t_o} \Pi_e(t, B, \vec{v})\, dt, \tag{11}$$

where $t_o - t_i$ is the atom transit time through the probe beam. This time is determined by the atom trajectory in the probe beam, i.e. by the velocity component perpendicular to the laser beam, v_x. To calculate the total fluorescence $\Upsilon(B)$, we averaged $I_e(B, \vec{v})$ over atom trajectories, i.e. over incident angles of an atom on the probe beam and over different atom velocities ($\vec{v}$ summation). v_z, the velocity component parallel to the laser beam, determines the Doppler shift in the laser frequency seen by an atom:

$$\Upsilon(B) = \sum_{\vec{v}} |\vec{v}| I_e(B, \vec{v}) W_b(T, |\vec{v}|), \tag{12}$$

where $|\vec{v}|$ accounts for atom flux through the laser beam. In equation (12),

$$W_b(T, v) = 4\pi \left(\frac{M}{2\pi kT}\right)^{3/2} v^2 e^{-Mv^2/2kT} \tag{13}$$

is the Maxwell–Boltzmann distribution, k is the Boltzmann constant, T is the temperature of rubidium vapor and M is the mass of an ^{87}Rb atom. We have found that the main contribution to the total fluorescence $\Upsilon(B)$ comes from atoms with small v_z. The range of velocities v_z contributing to the fluorescence increases with the laser beam intensity.

2.3. Results

Line shapes of probe transmission are given in figure 5 for various angles between the electric vectors of linearly

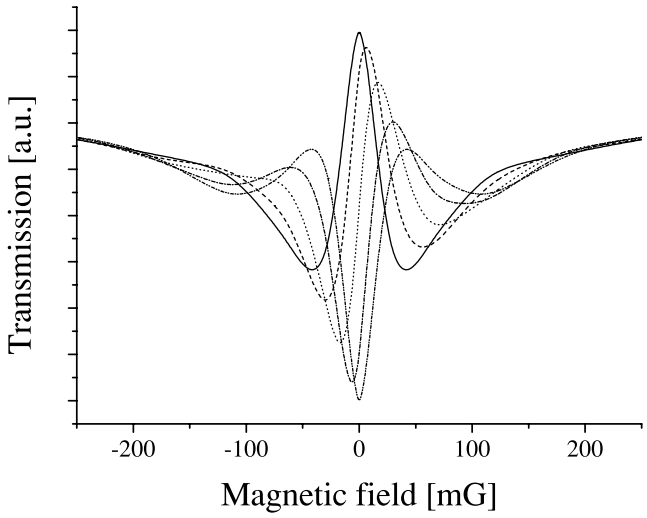

Figure 5. Calculated spontaneous emission as a function of the magnetic field for different probe beam polarization angles with respect to pump beam polarization (0° solid line, 20° dashed line, 45° dotted line, 70° dashed-dotted line, 90° dashed dot-dot line). Beam powers and dimensions are the same as in figure 2.

polarized pump and probe beams. Magnetic field, according to its strength, adds the phase to the dark state as the atom travels along the unlit region. Then the atom enters the probe with some accumulated phase. Polarization of the probe determines the accumulated phase and hence the magnetic field for which the atom–probe interaction is the strongest. Indeed, as the probe's polarization angle increases, the first transmission peak shifts towards higher values of B. Good agreement with preliminary experimental results has been achieved [7].

3. Conclusion

We have demonstrated dark Raman resonance due to Ramsey interference in spatially separated pump and probe beams. The pump and probe laser beams copropagate tuned to the $F_g = 2 \rightarrow F_e = 1$ transition D1 line in ^{87}Rb. These results are of interest for quantum optics of the dark states.

Acknowledgments

This work was supported by the Ministry of Science and Environmental Protection of the Republic of Serbia, under grant number 141003.

References

[1] Scully M O and Zubairy M S 1997 *Quantum Optics* (Cambridge: Cambridge University Press)
[2] Harris S E 1997 *Phys. Today* **50** 36
[3] Budker D, Yashchuk V and Zolotorev M 1998 *Phys. Rev. Lett.* **81** 5788
[4] Novikova I, Xiao Y, Phillips D F and Walsworth R L 2005 *J. Mod. Opt.* **52** 2381
[5] Briaudeau S, Saltiel S, Leite J R R, Oria M, Bramati A, Weis A, Bloch D and Ducloy M 2000 *J. Phys. IV France* **10** 145
[6] Harris M L, Adams C S, Cornish S L, McLeod I C, Tarleton E and Hughes I G 2006 *Phys. Rev.* A **73** 062509
[7] Grujić Z D, Mijailović M, Arsenović D, Kovačević A, Nikolić M and Jelenković B M 2008 *Phys. Rev.* A **78** 063816